Langmuir
Article
pubs.acs.org/Langmuir

Synthesis and Surface Properties of a pH-Regulated and pH-Reversible Anionic Gemini Surfactant

Jing Lv,[†] Weihong Qiao,*[,†] and Chongqiao Xiong[‡]

[†]State Key Laboratory of Fine Chemicals, School of Chemical Engineering, Dalian University of Technology, Dalian, 116024, P. R. China

[‡]College of Letters & Science, University of California, Berkeley, California 94720, United States

Supporting Information

ABSTRACT: A new series of *N,N*′-dialkyl-*N,N*′-diacetate ethylenediamine, differing by the length of the carbon tails (8, 10, and 12), was synthesized in two steps. Their surface properties and aggregation behavior were studied in aqueous solution using pH titration, surface tension, zeta potential, dynamic light scattering (DLS), transmission electron microscopy (TEM), and fluorescence measurements. On the basis of the pK_a values obtained, surface tension was measured, as well as key surface property parameters. Combined with the zeta potential and DLS results, the experiments produced vesicles and reflected their pH-controllability through subsequent TEM and fluorescence measurements. pH-switchability was found to be reversible by light transmittance. Emulsion stability of dodecane-in-water in different pH showed that emulsion type was reversed between "on" for the O/W emulsion type and "off" for the W/O.

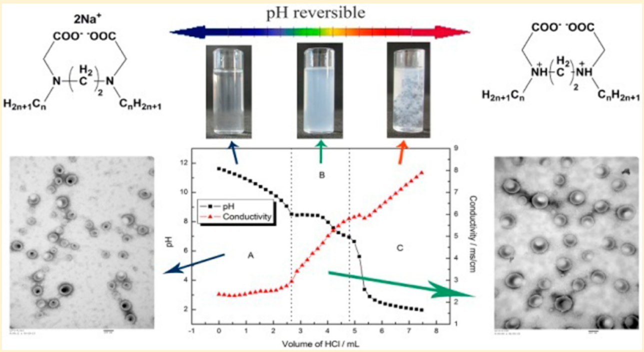

1. INTRODUCTION

Surfactants are widely used in many areas of the commercial and industrial world, which makes it seemingly unattractive for researchers to further investigate their structures.[1] The discovery of gemini (dimeric) surfactants reverses this point of view. Gemini surfactants are made up of two surfactant-like moieties connected at the level of the head groups or on the alkyl chains in close vicinity to the head groups by a spacer group of varying nature and length (see Scheme 1).[2] Due to their special structure, gemini surfactants are superior to the corresponding conventional monomeric surfactants in certain characteristics, such as remarkably low critical micellar concentration (CMC), high surface activity, low Krafft temperature, unusual rheological properties, multifarious aggregate structures, and better wettability.[3,4] Owing to these unique properties, gemini surfactants have attracted great attention in both academics and industry.

Scheme 1. Schematic Representation of a Gemini Surfactant with the Spacer Group Connecting (A) the Two Head Groups (Often the Case for Cationic Surfactants) and (B) he Alkyl Chains at a Location Very Close to the Head Groups (Case of Nonionic and Anionic Gemini Surfactants)

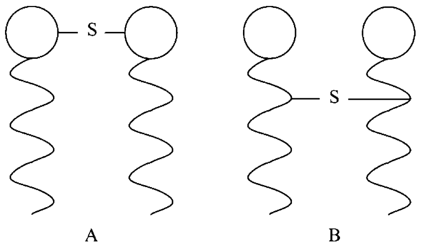

Similar to conventional surfactants, gemini surfactants are also classified into anionic,[5] cationic,[6] nonionic,[7] and zwitterionic gemini surfactants,[8] among which anionic gemini surfactants have an important place. The negative polar groups can be carboxylate,[9] sulfonate,[10] sulfate,[11] or phosphate;[12] and the spacer can be polar[13] or nonpolar, rigid or flexible.[14] Many types of anionic gemini surfactants have been synthesized and the investigation of their properties of cmc, surface tension, foaming, and wettability has been reported.[15,16] However, data are unable to show a sufficient relationship between the structures and properties of anionic gemini surfactants. Moreover, investigating properties such as aggregation number and size of anionic gemini surfactant micelles in solution is also critical.[17,18]

Surfactants are commonly known for forming micelles in solution. All the properties of the surfactant are built on the micelle. Micelles are in dynamic equilibrium, constantly disintegrating and reforming. As for the gemini surfactant, the spacer as an important factor affects the micelle behavior and

Received: October 9, 2013
Revised: June 20, 2014
Published: June 27, 2014

ACS Publications

dx.doi.org/10.1021/la5016669 | *Langmuir* 2014, 30, 8258−8267

thus cannot be ignored. The kinetics of exchange, size, and shape in micellar systems of cationic gemini surfactant of the alkanediyl-α,ω-bis(dodecyldimethylammonium bromide) type were studied,[19] with the alkanediyl being 1,2-ethylene, 1,3-propylene, and 1,4-butylene. Evidently, the results indicate that to obtain the truly unique properties of C_{12} cationic gemini surfactants, an ethylene spacer should be used. Vesicles are observed above the cmc for gemini surfactants. Wang et al.[20] extensively studied the aggregation behaviors of a series of anionic sulfonate gemini surfactants $[(C_nH_{2n+1})(C_3H_6SO_3^-)NC_sN(C_3H_6SO_3^-)(C_nH_{2n+1})]2Na^+$ and their corresponding monomeric surfactants. The gemini surfactants $C_{12}C_{px}C_{12}(SO_3)_2$ and $C_{12}C_3C_{12}(SO_3)_2$ exhibit a stronger aggregation ability in comparison with the monomeric surfactant $C_{12}NSO_3$. Zhu et al.[21] synthesized four sulfonate-containing gemini surfactants C_y-M_x-C_y. All the spacers of these gemini surfactants contained two rigid benzene rings and two rigid carbonyl groups. The aggregation behavior of C_7-M_x-C_7 in water was observed using DLS and typical TEM. The analyses proved that C_y-M_x-C_y with a long, fully rigid spacer preferred to form vesicles.

A number of studies[9,22−24] have focused on the synthesis of gemini surfactants with ethylenediamine as the spacer and carboxylate as the anionic group in the same molecule. A new type of gemini carboxylate surfactant based on EDTA was synthesized by Laurent Wattebled and André Laschewsky.[25] The existence of $N-CH_2COO^-$ groups implied that this kind of gemini surfactant existed in different forms in solution as a function of the pH, which were expressed as pK_{a1} and pK_{a2}. This indicated that the properties of this structure could be influenced by pH. In consideration of the nitrogen atom and carboxylate both able to combine with H^+, it can be predicted that the properties of such surfactants are controlled by pH. However, the surface adsorption and micellization characteristics in this field have seldom been reported.

Herein we focus on the synthesis and adsorption/micellization behavior of anionic gemini surfactants synthesized from ethylenediamine, Ace(*n*)-2-Ace(*n*) (*N,N*′-dialkyl-*N,N*′-diacetate ethylenediamine, where *n* is the hydrocarbon chain length with size 8, 10, and 12). The synthesis route and structure are shown in Scheme 2. This paper is focused on exploring the physicochemical properties of Ace(*n*)-2-Ace(*n*) at the air/water solution interface and in aqueous solution. The pK_a values are determined by acidic titration and all the property measurements, including surface tension, zeta potential, dynamic light scattering, transmission electron microscope, light transmittance, and fluorescence measurements, are conducted at different pH intervals.

Scheme 2. Synthetic Route of Ace(*n*)-2-Ace(*n*)[a]

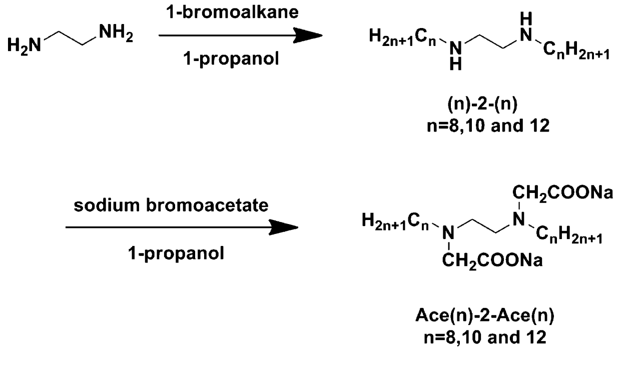

[a] *n* = 8, 10, and 12.

2. EXPERIMENTAL SECTION

2.1. Materials. For the synthesis of Ace(*n*)-2-Ace(*n*), ethylenediamine (Kermel Laboratory Equipment Co., Ltd.), 1-bromooctane, 1-bromodecane, 1-bromododecane (J&K Chemical, Ltd.), and bromoacetate acid (Sinopharm Chemical Reagent Co, Ltd) were used. Other reagents were methanol, 1-propanol, acetone, diethyl ether, and sodium hydroxide. The alkane used in the emulsion measurements was *n*-dodecane (Kermel Laboratory Equipment Co., Ltd.). The chemicals listed above were of analytical grade and used without further purification.

2.2. Synthesis. The final surfactants, Ace(*n*)-2-Ace(*n*) (*n* = 8, 10, and 12), were synthesized via the following two steps (see also Scheme 2). The products obtained in each step were characterized with mass spectrometry (High Performance Liquid Chromatography/Mass selective Detector, HP America, model HP1100LC/MSD), Accurate-Mass TOF LC/MS (Aglient 6224, Aglient Technology Inc.), ^1H NMR and ^{13}C NMR (Bruker, France, Model AVANCEII, 400 MHz), and FT-IR (Nicolet 6700 Flex FT-IR Spectrometer, Thermo Fisher Scientific). The synthesis details and structural characterization are described in the Supporting Information.

2.3. Measurements. The aqueous surfactant solutions were prepared via direct dissolution of the solid samples at the desired concentration. The surfactant solutions used in all the measurements (except emulsification) were all in a homogeneous phase. All the measurements were performed at 25 °C. Except for the acidic titration, surface tension, and emulsion, the sample concentration for all the other measurements was fixed at 10^{-3} mol/L.

2.3.1. Acidic Titration. Acidic titration of the anionic gemini surfactants was performed to determine the different species present in solution as a function of the varying pH. The surfactants were dissolved in excess of aqueous NaOH, the concentration was fixed at 0.01 M and the volume was 20 mL. The aqueous HCl concentration was 0.1 M. During the acidic titration, the changes of pH and conductivity were followed with a pH meter model (PHS-3C, Shanghai Hong Yi Instrumentation Co., Ltd) and with a conductivity meter (DDSJ-308A conductivity meter, Shanghai Hong Yi Instrument Co., Ltd.), respectively. The values of pK_a were fundamental for all the measurements. The following measurements were all conducted at different pH intervals in accordance with the pK_a.

2.3.2. Surface Tension. The surface tension was measured with Krüss K100C tensiometer. The cmc and the surface tension at the cmc were determined from the break point of the surface tension and the logarithm of the concentration curve. Repeated measurements were performed until the difference between two values was less than 0.2 mN/m.

2.3.3. Zeta Potential. The zeta potential was measured using Nanoparticle Zeta Potential Measurement (ZETASIZER nano series Nano ZS-90, Malvern, UK). The zeta potential is determined by the surface charge of aggregates formed by surfactant molecules in solution.[26] The pH values of all the samples corresponded to the samples in the test of surface tension. Each Ace(*n*)-2-Ace(*n*) at each pH was measured three times at 298 K.

2.3.4. Dynamic Light Scattering. All static light scattering measurements were performed on a Malvern autosizer (ZETASIZER nano series Nano ZS-90, Malvern, UK) at 90° scattering angle. All the samples were dispersed with ultrasound for 1 h. The obtained scattering data were fitted using an intensity-weighted cumulative analysis to estimate the diffusion coefficient of the aggregates in aqueous solution.[27] The average hydrodynamic diameter D_{ho} and the polydispersion index (PDI) of the solution were obtained.

2.3.5. Transmission Electron Microscopy. TEM micrographs were obtained with JEM-2000EX. Negative staining samples were prepared with phosphotungstic acid acetate solution (2%) as the staining agent. One drop of the solution was placed onto a carbon-coated copper TEM grid (300 mesh).[28] Filter paper was employed to suck away the

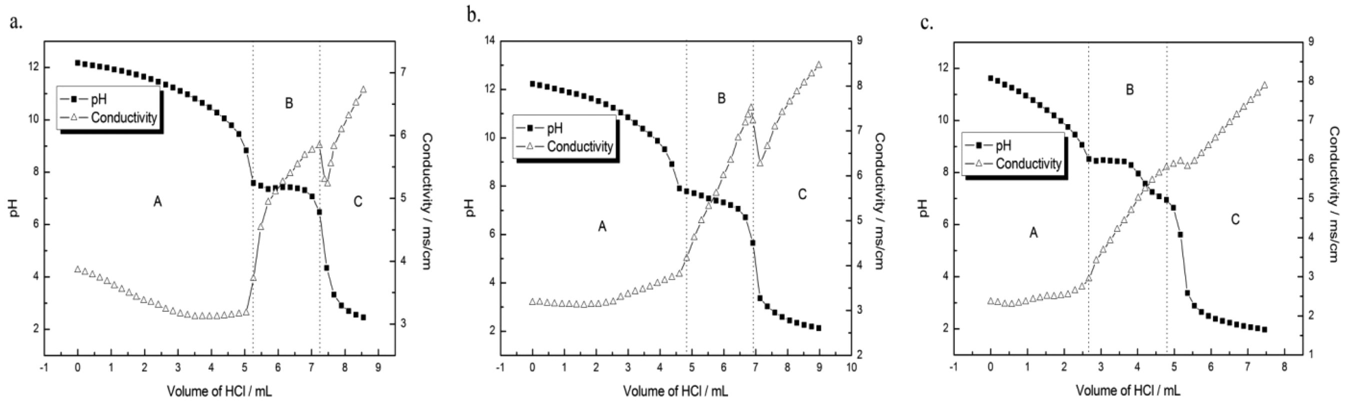

Figure 1. Acidic titration curves of Ace(*n*)-2-Ace(*n*): (a) Ace(8)-2-Ace(8); (b) Ace(10)-2-Ace(10); (c) Ace(12)-2-Ace(12).

Scheme 3. Transitions Occurring during the Titration of Gemini Surfactants with HCl

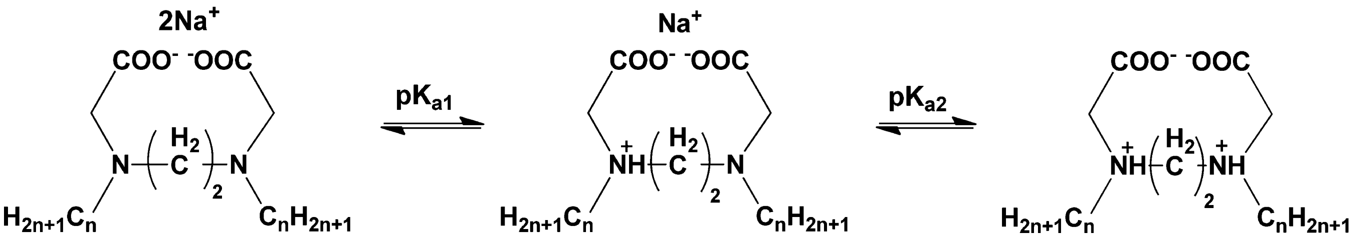

excess liquid. Then, one drop of the staining agent was placed onto the copper grid. Excess liquid was also sucked away by filter paper.

2.3.6. Fluorescence Measurements. Steady-state fluorescence spectra were recorded on HITACHI F-7000 Fluorescence Spectrophotometer. Pyrene was chosen as the fluorescent agent. The pyrene–surfactant binary solution was dispersed with ultrasound and kept overnight. The emission spectra wavelength ranged from 350 to 550 nm, and the excitation wavelength was focused at 335 nm.[29] Intensities of peaks labeled as I_1 and I_3 were taken from the emission intensities at 374 and 383 nm, respectively. Excitation and emission slits were fixed at 2.5 and 5 nm, respectively. The pyrene concentration was kept at 3×10^{-6} mol/L in the measurements to avoid excimer formation.

2.3.7. Light Transmittance. Light transmittance change with pH was measured on a Mettler ToledoT90 instrument. During the measurement, the pH and transmittance data were collected simultaneously. The original sample was dissolved in excess of NaOH and the pH was fixed at nearly 10. In one cycle test, the pH was adjusted from alkalinity to acidity (0.1 mol/L HCl was used) and then from acidity back to alkalinity (0.1 mol/L NaOH was used). This process was repeated at least three times in order to explore whether it could be reversible.

2.3.8. Emulsion Stability Measurements. Classical bottle tests were run to characterize the oil in water emulsion stability.[30] Ten milliliter surfactant solution and 10 mL alkane (dodecane) were added to a 100 mL beaker. Dispersion machine SFJ-400 was used to complete the emulsion process and the condition was 800 rpm for 10 min. Emulsion stability was determined by observing the emulsion that was held for 24 h. The whole process was completed in a water bath at 25 °C.

3. RESULTS AND DISCUSSION

3.1. Values of pK_a. The surfactant was dissolved in excess of a known NaOH solution, pH of 11−12. During the acidic titration, pH and conductivity data were collected at the same time. Titration curves obtained by addition of HCl (0.1 M) to surfactant solution as well as conductivity change are shown in Figure 1a,b,c. The dotted lines indicate a visual gradual change of the solution: transparent, turbid, and suspensions (corresponding to the section A, B, and C, respectively, in the figure). Each acid titration curve exhibits two turning points corresponding to two abrupt transition points of conductivity change.

With the addition of HCl in acidic titration, the concentrations of H^+ and Cl^- were increased resulting in conductivity increase up around the whole concentration. The appearance of these two breaking points demonstrated that there was a protonation between H^+ and the tertiary amine group in the surfactant molecule. The first turning point at pH around 8.00 corresponds to the addition of one proton to the anionic dimer. The second turning point at pH near 6.50 is attributed to the protonation of the second amine of the spacer group. The different equilibria involved in titration are schematized in Scheme 3. The change of the molecular structure of Ace(*n*)-2-Ace(*n*) with pH has been justified with FT-IR (Figure S4 in the Supporting Information, take Ace(12)-2-Ace(12) for example). From titration data, the protonation constants pK_{a1} and pK_{a2} were summarized in Table 1.

Table 1. Protonation Constants pK_{a1} and pK_{a2} of Ace(*n*)-2-Ace(*n*)

Gemini surfactants	pK_{a1}	pK_{a2}
Ace(8)-2-Ace(8)	7.59	7.02
Ace(10)-2-Ace(10)	7.83	6.59
Ace(12)-2-Ace(12)	8.41	6.55

As shown from the data in Table 1, three gemini surfactants have different pK_{a1} and pK_{a2} values. However, an obvious law can be inferred: as the hydrocarbon chain length increases, the value of pK_{a1} becomes higher and the value of pK_{a2} becomes lower, which means the range between pK_{a1} and pK_{a2} broadens. The impact this law would bring to the performance of Ace(*n*)-2-Ace(*n*) will be discussed in a later section.

3.2. Adsorption to the Air/Water Solution Surface. Figure 2a,b,c depicts the surface tension versus log concen-

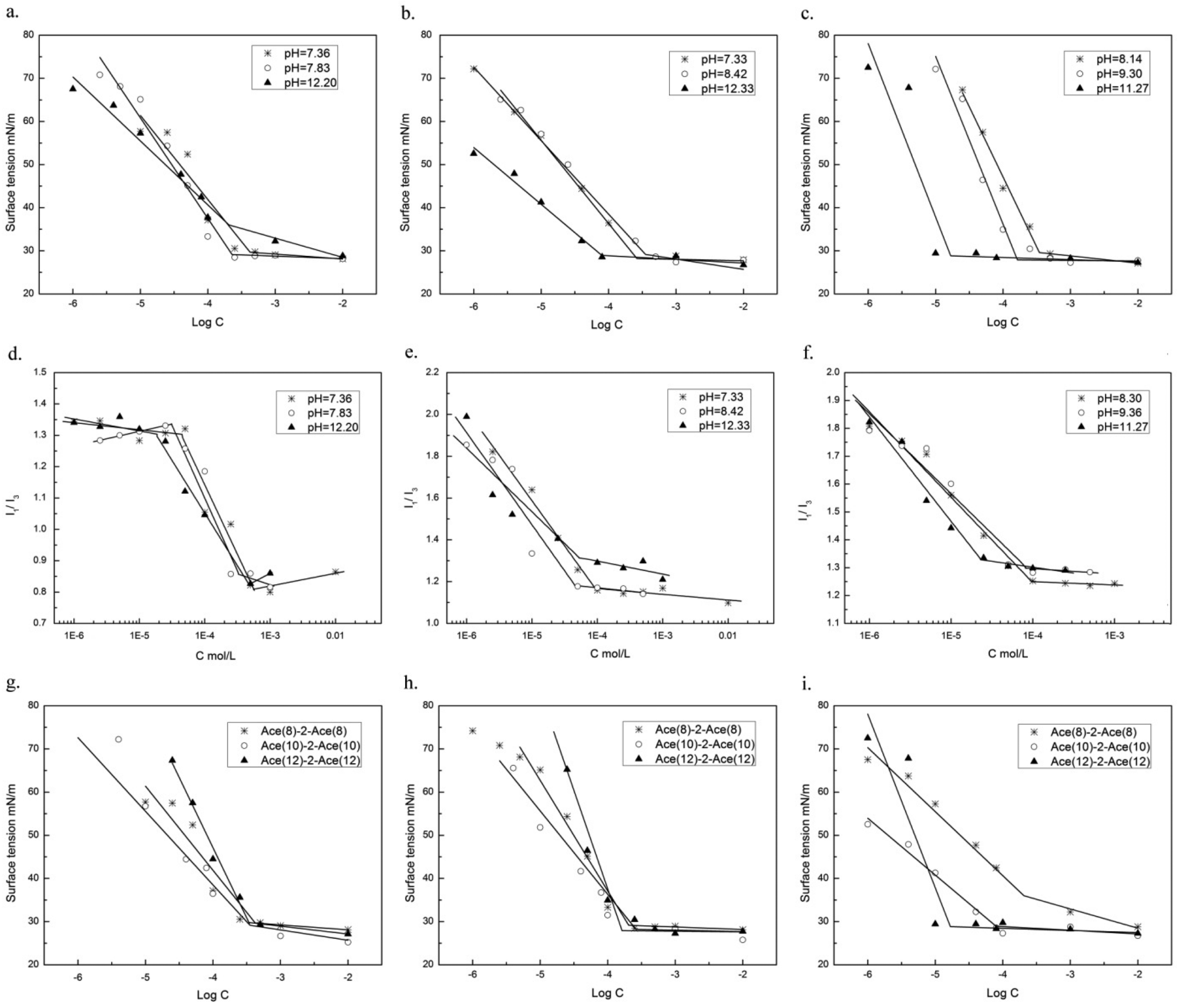

Figure 2. Six curves on surface tension versus log concentration and three curves on I_1/I_3 versus surfactant concentration: (a) and (d) Ace(8)-2-Ace(8); (b) and (e) Ace(10)-2-Ace(10); (c) and (f) Ace(12)-2-Ace(12); comparison between surface tension of aqueous Ace(*n*)-2-Ace(*n*) solution at different pH conditions: (g) pH^a, (h) pH^b, (i) pH^c.

tration plots for Ace(*n*)-2-Ace(*n*) (n = 8, 10, and 12) at three different pH intervals in accordance with the pK_a: between pK_{a1} and pK_{a2}, approximate pK_{a1} (pH is slightly higher than pK_{a1}), and far above pK_{a1} (for the sake of simplicity, use pH^a, pH^b, pH^c to represent these three pH intervals, respectively, similarly hereinafter). Table 2 lists the surface properties of Ace(*n*)-2-Ace(*n*) and some other common surfactants at 298 K. By contrast, the cmc of Ace(*n*)-2-Ace(*n*) is lower by more than one order of magnitude. Similarly, a significantly lower γ_{cmc} value is obtained as compared with that for the conventional surfactants. This can be ascribed to the characteristics in their molecule structures: two hydrophilic/hydrophobic groups are connected together by the chemical band in gemini surfactant, which overcomes the repulsive force between ions and the interaction force between alkyl chains to some extent. In addition, this effect brings adjacent hydrophilic groups closer, and simultaneously results in the distance between hydrophobic groups becoming smaller than in traditional surfactants. Therefore, there would be more alkyl hydrophobic chains arranged closely at the air/water interface of the gemini surfactant solution. Moreover, with the help of spacer, the alkyl chains tend to be presented in erected direction, leaving more methyl exposed to air. Because the surface energy of methyl is less than that of methylene, this kind of arrangement is supposed to confer higher surface activity to gemini surfactants. That is why Ace(*n*)-2-Ace(*n*) possesses a greater ability to reduce the surface tension of water. Besides, the adsorption and micellization of surfactant can also be expressed by the pC_{20} parameter. pC_{20} is the value of the logarithm of reciprocal C_{20}, which is concentration of surfactants leading to a decrease in the surface tension of water by 20 mN/m. The larger the pC_{20} value is, the higher the surface activity of surfactant is. The data showed that pC_{20} of Ace(*n*)-2-Ace(*n*) is always larger than that of traditional surfactants. As explained above, the compactness of both the adsorption on the interface and the micelles in the solution formed by gemini surfactant is greater due to the two alkyl chains. So, the double-chained Ace(*n*)-2-Ace(*n*) has

Table 2. Surface Properties of Ace(n)-2-Ace(n) and Some Other Common Surfactants at 298 K[g]

	cmc/mol/L		γ_{cmc}	Γ_{cmc}		A_o		ΔG°_{mic}	ΔG°_{ads}
	ST	FL	mN/m	μmol/m^2	R^2	Å^2	pC_{20}	kJ/mol	kJ/mol
Ace(8)-2-Ace(8)[a]	4.10×10^{-4}	5.00×10^{-4}	30.0	3.42	0.613	48.6	4.29	−10.5	−22.8
Ace(10)-2-Ace(10)[a]	3.53×10^{-4}	1.04×10^{-4}	29.6	3.13	0.994	53.1	4.77	−10.7	−24.4
Ace(12)-2-Ace(12)[a]	3.54×10^{-4}	1.00×10^{-4}	29.6	5.70	0.975	29.2	4.17	−10.7	−18.1
Ace(8)-2-Ace(8)[b]	2.77×10^{-4}	3.26×10^{-4}	29.1	3.64	0.937	45.6	4.52	−11.0	−22.8
Ace(10)-2-Ace(10)[b]	2.63×10^{-4}	5.00×10^{-5}	28.2	3.39	0.941	49.0	4.71	−11.1	−24.0
Ace(12)-2-Ace(12)[b]	1.31×10^{-4}	8.12×10^{-5}	27.9	8.82	0.962	18.8	4.10	−11.9	−16.9
Ace(8)-2-Ace(8)[c]	2.06×10^{-4}	5.54×10^{-4}	36.0	2.60	0.954	63.9	4.66	−11.4	−25.2
Ace(10)-2-Ace(10)[c]	4.93×10^{-5}	5.30×10^{-5}	31.5	2.57	0.997	64.6	5.92	−13.1	−28.9
Ace(12)-2-Ace(12)[c]	1.68×10^{-5}	2.28×10^{-5}	28.8	7.05	0.468	23.6	5.24	−14.5	−20.6
SDBS[d]	1.78×10^{-3}		35.1	3.26		51.0	3.72		
$C_{11}H_{23}COONa$[e]	2.0×10^{-2}		37.5	2.3		69.0	2.43		
SDS[e]	8.2×10^{-3}		32.5	3.16		53.0	2.5		
$C_{10}H_{21}N(CH_3)_2CH_2COO$[f]	1.80×10^{-2}		39.7	4.51		40.0	2.59		
$C_{12}H_{25}N(CH_3)_2CH_2COO$[f]	1.80×10^{-3}		36.5	3.57		46.5	3.56		

[a]pH[a]. [b]pH[b]. [c]pH[c]. [d]Ref 21. [e]Ref 24; $C_{11}H_{23}COONa$ was measured at pH = 10. [f]Ref 29. [g]cmc: critical micelles concentration in mol/L. γ_{cmc}: surface tension. Γ_{cmc} surface excess concentration. "ST" refers to surface tension measurement. A_o: area/surfactant molecule at the interface. pC_{20}: logarithm of reciprocal C_{20} (concentration of surfactants to lead to a decrease of in surface tension of water by 20 mN/m). ΔG°_{mic}: standard free energy of micellization. ΔG°_{ads}: standard free energy of adsorption. "FL" refers to fluorescence measurement. "R^2" means the correlation coefficient of the surface tension versus log concentration line.

higher effectiveness than single-chained surfactants on the adsorption and micellization.

To confirm the cmc of Ace(n)-2-Ace(n), the micellization of Ace(n)-2-Ace(n) at 298 K was investigated by steady-state fluorescence spectra. The fluorescence intensity ratio of the first to the third band I_1/I_3 for pyrene can be taken as a measure of the polarity of the microenvironment. When the micelles are formed, pyrene solubilized in water will be preferentially incorporated into the inner hydrophobic region of micelles, resulting in an abrupt change of the I_1/I_3 ratio. Figure 2d,e,f displays the I_1/I_3 ratio variation with the concentration of Ace(n)-2-Ace(n). The cmc values calculated by the inflection point of I_1/I_3 versus c curves are in agreement with those determined by surface tension measurement (Table 2).

Combining Figure 2 and data about cmc and pC_{20} in Table 2, we reached three conclusions. First, for each Ace(n)-2-Ace(n), the cmc value increases when the pH decreases; the cmc of Ace(12)-2-Ace(12) shows obviously bigger fluctuation than that of Ace(10)-2-Ace(10) (Figure 2b,c) and Ace(8)-2-Ace(8)'s cmc doesn't distinctly change (Figure 2a), reflected as its order of magnitude stays at 10^{-4} throughout the whole pH range. This phenomenon can be explained as the decrease of pH (or the adding of H^+) worsens the Ace(n)-2-Ace(n)'s solubility in water and results in the increase in cmc values. So, it can be perceived that Ace(8)-2-Ace(8) owns the strongest ability to adapt the change of pH, with Ace(10)-2-Ace(10) being second, and finally Ace(12)-2-Ace(12). This prediction can also be confirmed in Figure S6 (in the Supporting Information). Second, from the perspective of comparing results among Ace(n)-2-Ace(n)s: for each pH interval, it shows the expected increase in surface activity--lower cmc and lower γ_{cmc} values--with the increase in alkyl chain length. Third, pC_{20} value of Ace(n)-2-Ace(n) decreases as pH decreases, which shows a lower surface activity trend with decreasing pH. Similar to the cmc values, the change of pC_{20} values becomes greater with alkyl chain lengthening. This trend can be thought of as the screening effect caused by the excess of NaCl. So, both salt and pH effects are more obvious for longer chains.

According to the surface tension curves, surface excess concentration at the air/solution interface Γ can be calculated from the Gibbs equation

$$\Gamma_{cmc} = -\frac{1}{2.303nRT}\left(\frac{d\gamma}{d\log C}\right)_{T,P} \tag{1}$$

where R is the perfect gas constant, T is the absolute temperature, and C is concentration of surfactant solution. The solution was prepared with excess of NaOH, so n was taken as 1.[24] The surface area per surfactant molecule A_o can be calculated using the following equation

$$A_0 = \frac{1}{N_A\Gamma} \tag{2}$$

where N_A is Avogadro's number. A greater value of Γ or a smaller value of A_o means a denser arrangement of surfactant molecules at the air/water interface.

The standard free energy of micellization (ΔG°_{mic}) for ionic gemini surfactants can calculated by the equation[31]

$$\Delta G^\circ_{mic} = RT\left(\frac{1}{2} + \beta\right)\ln X_{cmc} - \left(\frac{RT}{2}\right)\ln 2 \tag{3}$$

where β is the apparent degree of counterion binding to the micelle/solution interface calculated from $\beta = 1 - \alpha$. Here α is taken as 1 for the present gemini surfactants because the surfactants dissolve into surfactant ions and counterions in sodium hydroxide solution. The standard free energy of adsorption (ΔG°_{ads}) at the air/water interface is calculated by the equation[32]

$$\Delta G^\circ_{ads} = \Delta G^\circ_{mic} - (\Pi_{cmc}/\Gamma) \tag{4}$$

where $\Pi_{cmc} = \gamma_0 - \gamma_{cmc}$, with γ_0 = surface tension of water. The values of ΔG°_{mic} and ΔG°_{ads} are listed in Table 2.

Recently, the calculation of area per molecule of surfactant through Gibbs adsorption equation has been questioned. Menger et al.[33−35] and Laven et al.[36] have argued about whether the Gibbs equation for analyzing surface tension data to obtain the surface excess is appropriate. In response to this

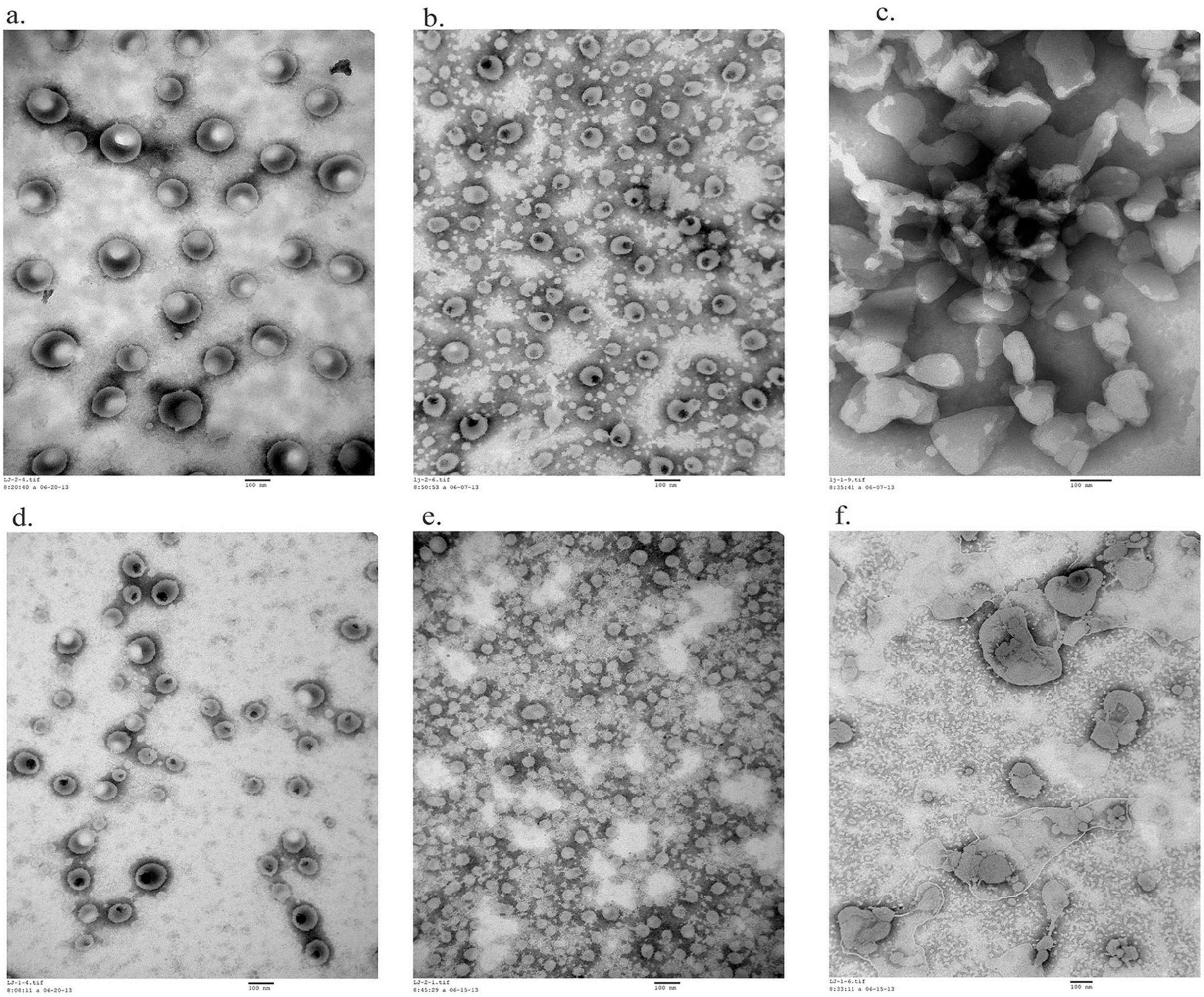

Figure 3. TEM micrographs of Ace(*n*)-2-Ace(*n*) at 10^{-3} mol/L. Bars in the photographs represent 100 nm: (a) Ace(8)-2-Ace(8)[a], (b) Ace(10)-2-Ace(10)[a], (c)Ace(12)-2-Ace(12)[a], (d) Ace(8)-2-Ace(8)[c], (e) Ace(10)-2-Ace(10)[c], and (f) Ace(12)-2-Ace(12)[c].

issue, two newest articles of Thomas[37,38] have provided the ensuing discussion about the application of the Gibbs equation to the air/water interface. It was pointed out in ref 38 that (i) the Gibbs equation cannot in principle be applied to an aqueous solution of ionic surfactant in the absence of electrolyte, (ii) impurities (mainly referring to divalent ion, i.e., Ca^{2+}, Mg^{2+}) present special difficulties for surface tension. If adsorption reached a plateau before the cmc, the analysis is straightforward and can be reasonably accurate. According to Thomas's research results, both measurements at higher concentrations and measurements using added electrolyte indicate that the adsorption of anionic surfactants has generally not reached a packing limit at the cmc. Several scholars[39−42] having analyzed the effect of a range of concentration of added NaCl on the surface tension of sodium dodecyl sulfate also supported Thomas's point. In this paper, all the aqueous systems in measurements contained excess NaCl which was brought in during sample preparation. So, the error caused by salts or impurities was uniform for three compounds. Furthermore, the Γ_{cmc} calculated from the constant slope of the surface tension vs the logarithm of the concentration curve was just used for qualitative analysis, not for further accurate calculation. The prediction obtained from the changing trend of Γ_{cmc} needs support from other data sources.

The values of Γ_{cmc} and γ_{cmc} under different pH conditions are also presented in Table 2. It is worth mentioning that the change of γ_{cmc} shows a related trend with Γ_{cmc}: the bigger Γ_{cmc} is, the lower γ_{cmc} is. It is reasonable that the bigger Γ_{cmc} means lower A_o and more tightly packed surfactant molecules arranged at the interface. It is the air/water interface becoming more nonpolar at higher Γ_{cmc} values that results in lower γ_{cmc}. More interestingly, Γ_{cmc} is the highest at pH[b] and the lowest at pH[c] (except for n = 12). As for Ace(12)-2-Ace(12), its Γ_{cmc} still shows the highest value at pH[b], but lowest at pH[a]. This tendency is caused by the decreasing solubility at lower pH condition. After all, the pH effect is more obvious for longer chains. Even so, the Γ_{cmc} values of Ace(12)-2-Ace(12) are still distinctly bigger than those of the other two Ace(*n*)-2-Ace(*n*)s, which once again demonstrates that longer chains have better adsorption at the air/water interface. Superficially, the reason for this result is the change of pH conditions, but in fact, it is caused by the change of intramolecular and intermolecular interaction due to the increased positive charge from the nitrogen atoms, and the intermolecular interaction can also be affected by alkyl chain. This is exactly what is meant by "structure determines performance". Although the solubility of Ace(*n*)-2-Ace(*n*) decreases with decreasing pH, which leads to higher cmc and lower pC_{20} values, the Γ_{cmc} values do not show consistent decrease with surface activity, but increase at the two

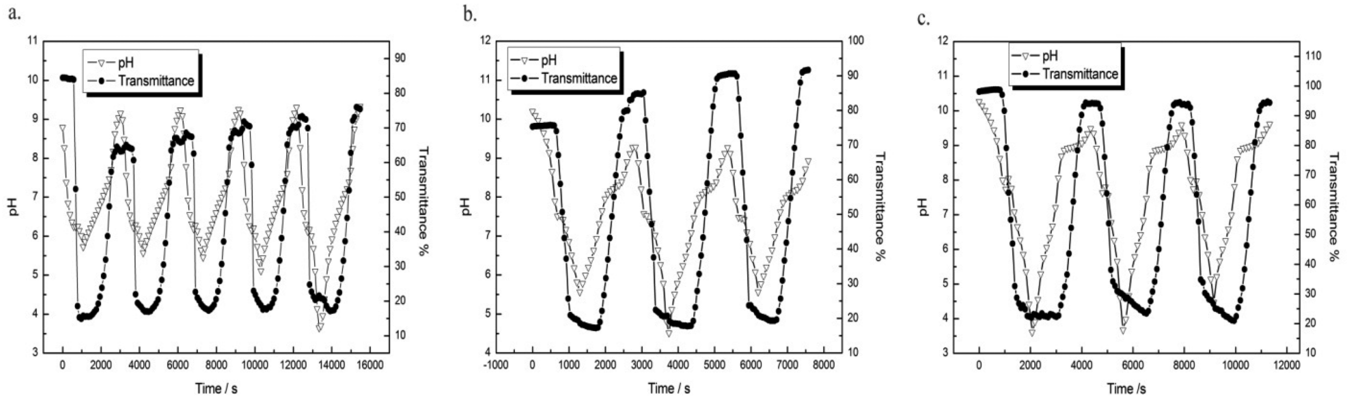

Figure 4. Transmittance of Ace(*n*)-2-Ace(*n*) solution as a function of time of treatment with HCl followed by NaOH solution: (a) Ace(8)-2-Ace(8), (b) Ace(10)-2-Ace(10), and (c) Ace(12)-2-Ace(12).

lower pH conditions. It shows a kind of balance between the solubility and adsorbability. Moreover, the effect of excess of NaCl cannot be ignored. It is these three impacts--alkyl chain length, pH, salt--functioning together that result in this changing law.

Figure S5 and subsequent description (in the Supporting Information) explain in detail the effect on the molecular structure brought about by change of pH conditions. To demonstrate this effect's reasonability, zeta potential was introduced to measure surface charge distribution of the aggregates formed by surfactant molecules. The results are shown in Table S1 of the Supporting Information.

Table S2 (in the Supporting Information) displayed a comparison Ace(*n*)-2-Ace(*n*)^c with some other reported gemini surfactants. The data shows that Ace(*n*)-2-Ace(*n*) is not inferior to any other gemini surfactant, and further proves that gemini surfactants truly possess a great effect on surface activity. Among those reported gemini surfactants, some owned similar structure to Ace(*n*)-2-Ace(*n*). As mentioned in the Introduction, the existence of N−CH_2COO^- groups indicated that the properties of this structure could be influenced by pH, but the surface adsorption and micellization characteristics in this field have seldom been reported. The above results show that pH indeed has a great influence on the performance of the Ace(*n*)-2-Ace(*n*) series. So, the following measurements for Ace(*n*)-2-Ace(*n*) were focused on alkaline (∼12.00) and neutral (∼7.50) properties in two distinct pH environments.

3.3. Aggregation Behavior in the Solution. During the zeta potential measurements, the prepared samples (concentration is 10^{-3} mol/L, at neutral pH) appeared bluish. Photograph of Ace(*n*)-2-Ace(*n*) in different pH environments is presented in Figure S6 (in the Supporting Information). As displayed in the photograph, with pH decreasing, the solution first appeared bluish and then precipitated as a white solid. From the point of view of appearance, Ace(12)-2-Ace(12) is most influenced by pH since the bluish just showed up at pH = 6.50 and surfactant completely precipitated at pH = 4.00; while under the same condition, the pH range for the bluish appearance is relatively wider for Ace(10)-2-Ace(10) and Ace(8)-2-Ace(8), especially for Ace(10)-2-Ace(10) (the bluish is still obvious at pH = 4.00). The disappearance of the bluish phenomenon and appearance of precipitation happened with the longest chain (*n* = 12), but not for shorter chains. This is confirmation of the pH effect on the alkyl chain, just as stated in section 3.2.

The solution showing a bluish tint suggests the existence of aggregate formed in solution. The aggregate can be micelle, vesicle, wormlike, or lamellae, so dynamic light scattering was further employed to study the aggregate size distributions of surfactant at 10^{-3} mol/L. The experimental results are presented in Figure S7 and Table S3 in the Supporting Information. As shown in Figure S7, only one distribution is detected in all of the investigated surfactant solutions at the neutral environment and two distinct distributions are observed in alkaline environment. Besides, PDI values in neutral environment are all smaller than those in the alkaline environment, which indicates that aggregates are better distributed in lower pH environment. Correspondingly, TEM measurements were carried out on the same surfactant solutions (the same concentration and the same sample preparation method). In Figure 3, spherical vesicles are found for all the surfactants and comparable aggregate numbers are shown. Similarly, the aggregate number in neutral environment is more than that at alkaline condition, except for Ace(10)-2-Ace(10), whose aggregate numbers in two pH environments show little difference. The DLS and TEM results can preliminarily prove that not only a better distribution but also a higher quantity of aggregate can be generated in Ace(*n*)-2-Ace(*n*) solutions under neutral pH environment.

To further demonstrate the change of aggregate number in Ace(*n*)-2-Ace(*n*) solutions, steady-state fluorescence spectra of pyrene−surfactant solution was measured. When the vesicles materialized, pyrene solubilized in water can be preferentially incorporated into the inner region of aggregates. The larger the aggregate quantity is, the greater the intensity of the fluorescence spectra. As shown in the fluorescence spectra of pyrene with varied surfactants and pure water (Figure S8 in the Supporting Information), the fluorescence intensity follows such a trend: Ace(12)-2-Ace(12)^a > Ace(10)-2-Ace(10)^a > Ace(8)-2-Ace(8)^a > Ace(8)-2-Ace(8)^c > Ace(10)-2-Ace(10)^c > Ace(12)-2-Ace(12)^c, which suggests the aggregate number is much bigger. The fluorescence intensity of pyrene-Ace(*n*)-2-Ace(*n*) solution at neutral pH is much stronger, which supports the TEM micrograph results.

3.4. pH-Responsive Reversibility Measurements. The results of the above measurements indicate that Ace(*n*)-2-Ace(*n*) are pH-responsive. During preparation of the samples for these measurements, the change in appearance of the solution with various pH values was observed: from totally transparent, bluish, and milky to finally a suspension. This change in appearance can be considered consistent with aggregate behavior in solution. Considering that this transformation is controlled by pH, we think the pH reversibility merits additional study. The reversibility and repeatability of the process were confirmed by monitoring the transmittance of the solution of Ace(*n*)-2-Ace(*n*) while HCl/NaOH solution was added into the solution over at least three cycles (Figure 4). In the first cycle, transmittance diminished when HCl was titrated and reached a plateau region, then it rose upon NaOH addition. Based on the first cycle, the same process was repeated for two more cycles (four for Ace(8)-2-Ace(8)). There are some differences among the reversible measurement results of three Ace(*n*)-2-Ace(*n*): (1) for $n = 8$, the transmittance cannot recover to the original state in the repeated cycles (the data decayed from 84.5% to 63.0%), and the maximum transmittance increases in the repeated cycle as the cycle number grows (63.0%, 65.7%, 68.5%, 70.1%, respectively); (2) for $n = 10$, far from reduction, the transmittance maximum increases all along (from 75.3%, 80.5%, 86.8%, to 90.6%); (3) for $n = 12$, the transmittance maximum also appears attenuated but remains comparatively stable; the degree of transmittance maximum attenuation is smaller than that of Ace(8)-2-Ace(8) (from the original value 98.2% to 94.3%, 94.5%, 94.7%, respectively).

From pH-responsive reversibility results, the difference among Ace(*n*)-2-Ace(*n*) should be attributed to a different sensitivity to salinity. The added volume of HCl or NaOH solution during each cycle was merely 1 mL, so the change in surfactant concentration can be ignored for the measured 40 mL solution. However, considering that the excess NaOH existed in the original solution, the concentration of NaCl after the first round of HCl addition became a factor that could not be neglected, not to mention that it had gradually increased in the following cycles. From the discussion in the previous paragraph, it seems that NaCl indeed plays an important role in affecting the aggregation behavior of Ace(*n*)-2-Ace(*n*). The increase in transmittance for surfactants with shorter chains ($n = 8, 10$) after repeated HCl/NaOH cycles means a disaggregation effect due to the increased concentration of Na^+ and Cl^-. The long-chained Ace(12)-2-Ace(12) are protected against the disaggregation due to the strong hydrophobic interaction of dodecyl.

3.5. Emulsion-Type Conversion. As we previously discussed, aqueous Ace(*n*)-2-Ace(*n*) solution presented different aspects at three different pH environments (transparent, semitransparent, and milky), but the solution is always homogeneous. Knowing that surface adsorption of Ace(*n*)-2-Ace(*n*) is pH-dependent, we then tested the stability of the dodecane-in-water emulsion prepared at different pH values. One thing we need to emphasize is that all the samples used were from the same batch as those used for surface tension measurements. This proves a strong correspondence to the previous results of surface tension.

Figure 5 is the photographs of dodecane-in-water prepared with Ace(*n*)-2-Ace(*n*) and stabilized after 24 h. The transformation of the emulsion type was patently exhibited. O/W emulsion was generated in the first two different pH environments, namely, pH^c and pH^b, while W/O emulsion was formed for pH^a. The double phase inversion is also supported by comparing the emulsion conductivities (as given in Table S4 in the Supporting Information). This characteristic provides a kind of pH-controllable surfactant, which not only controls the on-and-off aspect of the emulsion, but also reveals an environmentally friendly feature. Unfortunately, single Ace(*n*)-2-Ace(*n*) is not a good emulsifier, for demulsification happened within 24 h. So, further work in this area will include improvement of compounding Ace(*n*)-2-Ace(*n*) and other additives. The target is to develop a perfect temporary emulsifier which is obtained when switching "on" the O/W emulsion type of Ace(*n*)-2-Ace(*n*) and can be broken by switching it "off" to the W/O type. The additives can be other kinds of surfactants, nanoparticles, or polymers.

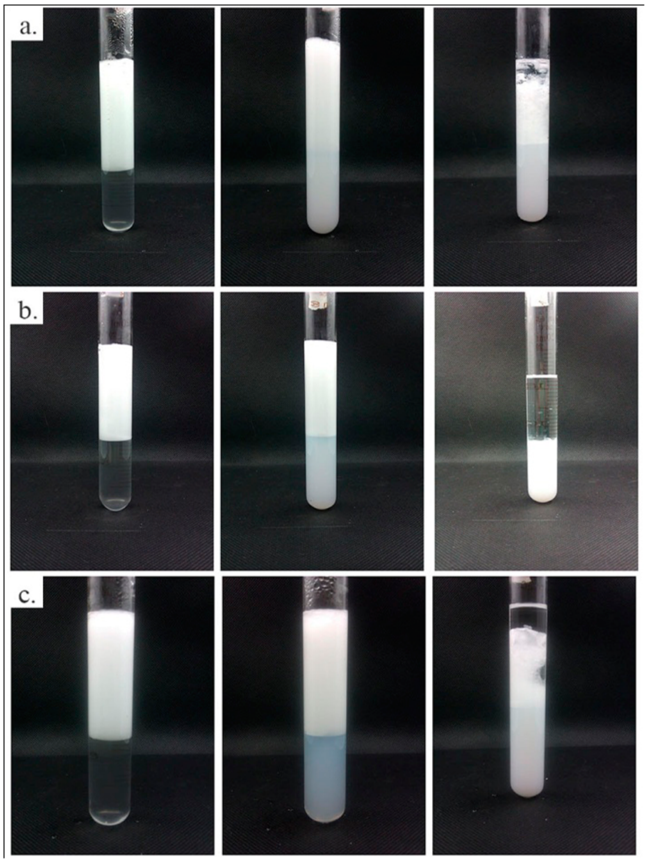

Figure 5. Photographs of 1:1 (v/v) dodecane/water mixtures containing 10^{-2} mol/L Ace(*n*)-2-Ace(*n*) at different pH values after 10 minutes of stirring followed by a waiting period of 24 h. From left to right, pH values are as follows: (a) Ace(8)-2-Ace(8), 11.47, 8.10, 7.50; (b) Ace(10)-2-Ace(10), 11.76, 8.42, 7.26; (c) Ace(12)-2-Ace(12), 11.60, 9.34, 8.15.

4. CONCLUSIONS

In this work, gemini surfactants Ace(*n*)-2-Ace(*n*) ($n = 8, 10, 12$) were synthesized and their characterization has been confirmed by Accurate-Mass Spectrum, ^1H NMR, and ^{13}C NMR. Ace(*n*)-2-Ace(*n*) existed in different forms in solution as a function of pH, expressed as $pK_{a1}$and pK_{a2}. Surface properties were systematically investigated in these three different pK_a intervals (far above pK_{a1}, near pK_{a1} and between pK_{a1} and pK_{a2}) at 298 K by several combined techniques. A series of useful parameters were obtained to evaluate their surface activity. The results indicate that Ace(*n*)-2-Ace(*n*) has far superior surface activity than traditional surfactants depending on much lower cmc/γ_{cmc} and higher pC_{20} values. The pH, alkyl chain, and excess of NaCl have great impact on the properties of Ace(*n*)-2-Ace(*n*). By analyzing the results of measurement, conclusions can be drawn about the changing law on the performance of the Ace(*n*)-2-Ace(*n*) series as follows. (1) The surface activity of

Ace(n)-2-Ace(n) increases with the increase in alkyl chain length. The longer the alkyl chain is, the more conspicuous the effects from pH and NaCl will be, reflected as the surface tension showing obvious fluctuation at $n = 12$ and not at $n = 10$ and 8; for each Ace(n)-2-Ace(n), cmc increases and pC_{20} decreases with decreasing pH, and the change is also more obvious for longer chains; the bluish phenomenon is obviously shorter lived for Ace(12)-2-Ace(12) than the other two Ace(n)-2-Ace(n)s. (2) pH can control the adsorption of Ace(n)-2-Ace(n) at the air/water interface and aggregation behavior in bulk solution: the Γ_{cmc} reaches a maximum at pH near pK_{a1}; aggregation becomes much greater at pH between pK_{a1} and pK_{a2}, supported by TEM and fluorescence intensity. Neutral pH makes much more and better distributed aggregates generated in Ace(n)-2-Ace(n) solution. (3) pH-controllability is reversible, verified by cycled transmittance measurements. Finally, from the standpoint of practical application, pH-responsive emulsion type conversion was described. With pH changing from alkaline to neutral, the emulsion type reverses from O/W to W/O. Considering the transmittance's reversibility, the emulsion's conversion shall also be repeatable. Many industrial applications relying on emulsions would benefit from this efficient, rapid method to produce switchable surfactants based on pH-responsivity.

■ ASSOCIATED CONTENT

Ⓢ Supporting Information

Synthesis and chemical characterization, schematic diagram on effect on molecular structure brought about by the change of pH, zeta potential of aqueous Ace(n)-2-Ace(n) solution at 10^{-3} mol/L, comparison of Ace(n)-2-Ace(n) with other reported gemini surfactants, photograph of Ace(n)-2-Ace(n) solution at 10^{-3} mol/L, DLS results of Ace(n)-2-Ace(n) at 10^{-3} mol/L, fluorescence spectra of pyrene−surfactant solution, conductivity (κ) of 1:1 (v/v) emulsion of dodecane and 10^{-2} mol/L Ace(n)-2-Ace(n) at different pH values. This material is available free of charge via the Internet at http://pubs.acs.org.

■ AUTHOR INFORMATION

Corresponding Author

*E-mail: qiaoweihong@dlut.edu.cn; fax: +86-0411-84986232.

Author Contributions

The manuscript was written through contributions of all authors. Initial conception, design, provision of resources, collection of data, analysis, interpretation of data and manuscript writing were completed by Jing Lv; Prof. Weihong Qiao provided theoretical guidance; Chongqiao Xiong made substantial contributions to writing and revising paper. All authors have given approval to the final version of the manuscript.

Notes

The authors declare no competing financial interest.

■ ACKNOWLEDGMENTS

This work was financially supported by Petro China Daqing Oilfield Co. Ltd. (DQYT-0508003-2011-JS-362). Dalian University of Technology Chemistry Analysis & Research Center is acknowledged for providing measurement instruments.

■ REFERENCES

(1) Menger, F.M.; Keiper, J.S. Gemini Surfactants. *Angew. Chem., Int. Ed.* **2000**, *39*, 1906−1920.

(2) In, M.; Zana, R. Phase Behavior of Gemini Surfactants. *J. Dispersion Sci. Technol.* **2007**, *28*, 143−154.

(3) Han, Y.H.; Wang, Y.L. Aggregation Behavior of Gemini Surfactants and Their Interaction with Macromolecules in Aqueous Solution. *Phys. Chem. Chem. Phys.* **2011**, *13*, 1939−1956.

(4) Sakai, K.; Sakai, H.; Abe, M. Recent Advances in Gemini Surfactants: Loeic Acid-based Gemini Surfactants and Polymerizable Gemini Surfactants. *J. Oleo Sci.* **2011**, *60* (4), 159−163.

(5) Shukla, D.; Tyagi, V.K. Anionic Gemini Surfactants: A Distinct Class of Surfactants. *J. Oleo Sci.* **2006**, *55* (5), 215−226.

(6) Zana, R.; Benrraou, M.; Rueff, R. Alkanediyl-*α*, *ω*-bis-(dimethylalky1ammonium bromide) Surfactants. 1. Effect of the Spacer Chain Length on the Critical Micelle Concentration and Micelle Ionization Degree. *Langmuir* **1991**, *7*, 1072−1075.

(7) Yoshimura, T.; Ishihara, K.; Esumi, K. Sugar-based Gemini Surfactants with Peptide Bonds-synthesis, Adsorption, Micellization, and Biodegradability. *Langmuir* **2005**, *21*, 10409−10415.

(8) Xie, Z.F; Feng, Y.J. Synthesis and Properties of Alkylbetain Zwitterionic Gemini Surfactants. *J. Surfactants Deterg.* **2010**, *13* (1), 51−57.

(9) Xu, J.; Liu, X.J.; Wang, B.; Qiao, Z.J. Synthesis and Characterization of Sodium N,N′-dioctyl-ethylenediamine Dicayl Propionate. *Int. J. Chem. (Toronto, ON, Can.)* **2010**, *2*, 194−197.

(10) Sakai, K.; Kaji, M.; Takamatusu, Y.; Tsuchiya, K.; Torigoe, K.; Tsubone, K.; Yoshimura, T.; Esumi, K.; Sakai, H.; Abe, M. Fluorocarbon−Hydrocarbon Gemini Surfactant Mixtures in Aqueous Solution. *Colloids Surf., A* **2009**, *333*, 26−31.

(11) Zhu, Y.P.; Masuyama, A.; Okahara, M. Preparation and Surface Active Properties of Amphipathic Compounds with Two Sulfate Groups and Two Lipophilic Alkyl Chains. *J. Am. Oil Chem. Soc.* **1990**, *67*, 459−461.

(12) Duivenvoorde, F.L.; Feiters, M.C.; Van der Gaast, S.J.; Engberts, J. B. F. N. Synthesis and Properties of Di-*n*-dodecyl-*α*, *ω*-Alkyl Bisphosphate Surfactants. *Langmuir* **1997**, *13*, 3737−3743.

(13) Sommerdijk, N. A. J. M.; Hoeks, T. H. L.; Synak, M.; Feiters, M.C.; Nolte, R. J. M.; Zwanenburg, B. Stereodependent Fusion and Fission of Vesicles: Calcium Binding of Synthetic Gemini Phospholipids Containing Two Phosphate Groups. *J. Am. Chem. Soc.* **1997**, *119*, 4338−4344.

(14) Song, L.D.; Rosen, M.J. Surface Properties, Micellization, and Premicellar Aggregation of Gemini Surfactants with Rigid and Flexible spacers. *Langmuir* **1996**, *12*, 1149−1153.

(15) You, Y.; Wu, X.N.; Zhao, J.X.; Ye, Y.Z.; Zou, W.S. Effect of Alkyl Tail Length of Quaternary Ammonium Gemini Surfactants on Foaming Properties. *Colloids Surf., A* **2011**, *384*, 164−171.

(16) Kuo, C.J.; Lin, L.H.; Dong, M.Y.; Chang, W.S.; Chen, K.M. Preparation and Properties of New Ester-Linked Cleavable Gemini Surfactants. *J. Surfactants Deterg.* **2011**, *14*, 195−201.

(17) Feng, J.; Liu, X.P.; Zhang, L.; Zhao, S.; Yu, J.Y. Preparation and Properties of New Ester-Linked Cleavable Gemini Surfactants. *Langmuir* **2010**, *26* (14), 11907−11914.

(18) Zana, R. Dimeric and Oligomeric Surfactants. Behavior at Interfaces and in Aqueous Solution: a Review. *Adv. Colloid Interface Sci.* **2002**, *97*, 205−253.

(19) Groth, C.; Nyden, M.; Holmberg, K.; Kanicky, J.R.; Shah, D.O. Kinetics of the Self-Assembly of Gemini Surfactants. *J. Surfactants Deterg.* **2004**, *7* (3), 247−255.

(20) Wang, Y.X.; Han, Y.C.; Huang, X.; Cao, M.W.; Wang, Y.L. Aggregation Behaviors of a Series of Anionic Sulfonate Gemini Surfactants and Their Corresponding Monomeric Surfactant. *J. Colloid Interface Sci.* **2008**, *319*, 534−541.

(21) Zhu, D.Y.; Chen, F.; Chen, Y.; Jiang, S.C. Preparation, Characterization and Properties of Anionic Gemini Surfactants with Long Rigid or Semi-rigid Spacers. *Colloids Surf., A* **2012**, *397*, 1−7.

(22) Frost, A.E., Jr.; Martell, E. The Preparation and Properties of Some N,N′-Dialkylethylenediaminediacetic Acids. *J. Am. Chem. Soc.* **1950**, *76*, 3743−3746.

(23) Sakai, K.; Umezawa, S.; Tamura, M.; Takamatusu, Y.; Tsuchiya, K.; Torigoe, K.; Tsubone, K.; Ohkubo, T.; Yoshimura, T.; Esumi, K.; Sakai, H.; Abe, M.; Sakai, K. Adsorption and Micellization Behavior of Novel Gluconamide-type Gemini Surfactants. *J. Colloid Interface Sci.* **2008**, *318*, 440−448.

(24) Yoshimura, T.; Esumi, K. Synthesis and Surface Properties of Anionic Gemini Surfactants with Amide Groups. *J. Colloid Interface Sci.* **2004**, *276*, 231−238.

(25) Wattebled, L.; Laschewsky, A. New Anionic Gemini Surfactant Based on EDTA Accessible by Convenient Synthesis. *Colloid Polym. Sci.* **2007**, *285*, 1387−1393.

(26) Leonard, I.A.; Gerard, R. Micellization of pH-stimulable Poly(2-vinylpyridine)-b-poly(ethylene oxide) Copolymers and Their Complexation with Anionic Surfactants. *J. Colloid Interface Sci.* **2013**, *395*, 190−197.

(27) Ngo, T. H. V.; Damas, C.; Naejus, R.; Coudert, R. Aggregation of New Bipolar Glucosyled and Cationic Fluoroamphiphiles in Aqueous Media. *J. Colloid Interface Sci.* **2013**, *389*, 157−163.

(28) Lin, Y.Y.; Han, X.; Cheng, X.H.; Huang, J.B.; Liang, D.H.; Yu, C. pH-Regulated Molecular Self-Assemblies in a Cationic-Anionic Surfactant System: From a “1-2” Surfactant Pair to a “1-1” Surfactant Pair. *Langmuir* **2008**, *24*, 13918−13924.

(29) Wang, X.Q.; Liu, J.; Yu, Li; Jiao, J.J.; Wang, R.; Sun, L.M. Surface Adsorption and Micelle Formation of Imidazolium-based Zwitterionic Surface Active Ionic Liquids in Aqueous Solution. *J. Colloid Interface Sci.* **2013**, *391*, 103−110.

(30) Argillier, J.F.; Zeilinger, S.; Roche, P. Enhancement of Aqueous Emulsion and Foam Stability with Oppositely Charged Surfactant/Polyelectrolyte Mixed Systems. *Oil & Gas Science and Technology* **2009**, *64* (5), 597−605.

(31) Zana, R. Critical Micellization Concentration of Surfactants in Aqueous Solution and Free Energy of Micellization. *Langmuir* **1996**, *12*, 1208−1211.

(32) Rosen, M.J.; Aronson, S. Standard Free Energies of Adsorption of Surfactants at the Aqueous/solution/air Interface From Surface Tension Data in Vicinity of the Critical Micelle Concentration. *Colloids Surf.* **1981**, *3* (3), 201−208.

(33) Menger, F. M.; Shi, L.; Rizvi, S. A. A. Re-evaluating the Gibbs Analysis of Surface Tension at the Air/Water Interface. *J. Am. Chem. Soc.* **2009**, *131*, 10380−10381.

(34) Menger, F. M.; Rizvi, S. A. A.; Shi, L. Reply to “Should the Gibbs Analysis Be Revised? *Langmuir* **2011**, *27*, 7963−7965.

(35) Menger, F. M.; Shi, L.; Rizvi, S. A. A. Additional Support for a Revised Gibbs Analysis. *Langmuir* **2010**, *26* (3), 1588−1589.

(36) Laven, J.; De.With, G. Should the Gibbs Analysis Be Revised? *Langmuir* **2011**, *27*, 7958−79622.

(37) Li, P. X.; Li, Z. X.; Shen, H.; Thomas, R. K.; Penfold, J.; Lu, J. R. Application of the Gibbs Equation to the Adsorption of Nonionic Surfactants and Polymers at the Air-Water Interface: Comparison with Surface Excesses Determined Directly using Neutron Reflectivity. *Langmuir* **2013**, *29*, 9324−9334.

(38) Xu, H.; Li, P. X.; Ma, K.; Thomas, R. K.; Penfold, J.; Lu, J. R. Limitations in the Application of the Gibbs Equation to Anionic Surfactants at the Air/Water Surface: Sodium Dodecylsulfate and Sodium Dodecylmonooxyethylenesulfate Above and Below the CMC. *Langmuir* **2013**, *29*, 9335−9351.

(39) Matuura, R.; Kimizuka, H.; Yatsunami, K. The Study of the Adsorption of Detergents at a Solution-air Interface by Radiotracer Method. III. The Effect of Inorganic Electrolytes on the Adsorption of Sodium Dodecyl Sulfate. *Bull. Chem. Soc. Jpn.* **1959**, *32*, 646−650.

(40) Tajima, K. Radiotracer Studies on Adsorption of Surface Active Substance at Aqueous surface. II. The Effects of Excess Salt on the Adsorption of Sodium Dodecylsulfate. *Bull. Chem. Soc. Jpn.* **1970**, *43*, 3063−3066.

(41) Hall, D. G.; Pethica, B. A.; Shinoda, K. The Interpretation of Surface Tension Data for Solutions of Ionic Surfactants In the Presence of Electrolyte. *Bull. Chem. Soc. Jpn.* **1975**, *48*, 324−326.

(42) Gurkov, T. D.; Dimitrova, D. T.; Marinova, K. G.; Bilke-Crause, C.; Gerber, C.; Ivanov, I. B. Ionic Surfactants on Fluid Interfaces: Determination of the Adsorption; Role of the Salt and the Type of the Hydrophobic Phase. *Colloids Surf., A* **2005**, *261*, 29−38.